Inorganic Chemistry
Article

Inorg. Chem. **2009**, *48*, 9005–9017 **9005**
DOI: 10.1021/ic901390n

Building Blocks for Molecule-Based Magnets: Radical Anions and Dianions of Substituted 3,6-Dimethylenecyclohexane-1,2,4,5-tetrones as Paramagnetic Bridging Ligands

Andrzej W. Misiołek,[†] Andrew S. Ichimura,[‡] Robert A. Gentner, Rui H. Huang, Vanessa P. McCaffrey,*[,§] and James E. Jackson*

Department of Chemistry, Michigan State University, East Lansing, Michigan 48824. [†]*Current address: "Sulima" Sp. z o.o., Esperanto 14a/26, 01-049 Warszawa, Poland.* [‡]*Current address: Department of Chemistry and Biochemistry, San Francisco State University, 1600 Holloway Avenue, San Francisco, CA 94132.* [§]*Department of Chemistry, Albion College, Albion, MI 49224.*

Received July 20, 2009

We have prepared four tetraaryl derivatives of 3,6-dimethylene-1,2,4,5-tetraoxocyclohexane (aryl = Ph; 4-MeOPh; 4-Me_2NPh; and 3,5-(*t*-Bu)$_2$-4-MeOPh) with guidance from an earlier reported ab initio analysis (Misiolek, A. W.; Jackson, J. E. *J. Am. Chem. Soc.* **2001**, *123*, 4774−4780). These electron acceptors may be chemically or electrochemically reduced to the mono- and dianions desired as building blocks for the assembly of molecule-based magnets. Cyclic voltammetry shows that the potential of the first reduction wave depends on the electron donor ability of the aryl ring substituents, ranging from −0.28 V for the tetraphenyl derivative to −0.78 V for the *p*-dimethylamino substituted analogue (vs ferrocene/ferrocinium$^+$ at 0.46 V). Spin density distributions in the semiquinone moieties were elucidated by electron paramagnetic resonance (EPR) and electron−nuclear double resonance (ENDOR) observations of hyperfine couplings to internal ^{1}H sites and bound alkali metal cations. X-ray diffraction studies of the sodium and potassium salts of the octa-*t*-butyltetramethoxy derivative reveal the structure of the monoanion and its tendency to self-assemble with metal cations into one-dimensional chains in the solid state. Within the chains the anions display the expected bridging and chelating mode of coordination; SQUID magnetometry revealed weak intermolecular spin−spin couplings of $2J = -0.2$ and ∼0 K for the sodium and potassium salts, respectively. NIR transitions in the electronic spectra of the monoanions in solution are consistent with the expected low energy gap between frontier orbitals and its tunability by substituent variations. EPR studies of the free dianions and monoradical analogues indicate diradical localization into separate triphenylmethyl-like monoradicals via twisting of the diarylmethylene termini.

Introduction

The use of organic molecules as components of magnetic materials promises rational control over their structural and magnetic properties.[1] One of the strategies for assembly of molecule-based magnets is a hybrid "metal-radical" approach in which organic radicals are combined with paramagnetic metal cations.[2] The main advantage of this approach over those utilizing diamagnetic organic components is direct intermolecular spin−spin contact, which promises robust magnetic interactions. Until recent years, the biggest challenge to this approach was the low diversity of available building blocks. Early studies focused on simple nitroxyls, the one general class of stable free radicals capable of significant spin contact with its environment. Though weak ligands, these radicals have proved capable of coordinating and magnetically coupling to a variety of metal centers.[3] Extension to bidentate radical partners allowed construction of one-dimensional (1-D) coordination polymers, most notably those between the neutral nitronyl nitroxides and the

*To whom correspondence should be addressed. E-mail: jackson@chemistry.msu.edu (J.E.J.), vmccaffrey@albion.edu (V.P.M.).

(1) (a) Kahn, O. *Molecular Magnetism*; VCH: New York, 1993. (b) *Magnetism: Molecules to Materials*; Miller, J. S., Drillon, M., Eds.; Wiley-VCH: Weinheim, 2001. (c) Miller, J. S.; Epstein, A. J. *Angew. Chem., Int. Ed. Engl.* **1994**, *33*, 385. (d) Gatteschi, D. *Adv. Mater.* **1994**, *6*, 635. (e) Rajca, A. *Chem. Rev.* **1994**, *94*, 871. (f) Iwamura, H. *Pure Appl. Chem.* **1987**, *59*, 1595.

(2) (a) Caneschi, A.; Gatteschi, D.; Rey, P. *Prog. Inorg. Chem.* **1991**, *39*, 331. (b) Caneschi, A.; Gatteschi, D.; Sessoli, R.; Rey, P. *Acc. Chem. Res.* **1989**, *22*, 392. (c) Lemaire, M. T. *Pure Appl. Chem.* **2004**, *76*, 277.

(3) (a) Alberola, A.; Coronado, E.; Giménez-Saiz, D.; Gómez-García, C. J.; Romero, F. M.; Tarazón, A. *Eur. J. Inorg. Chem.* **2005**, 389. (b) Fegy, K.; Sanz, N.; Luneau, D.; Belorizky, E.; Rey, P. *Inorg. Chem.* **1998**, *37*, 4518. (c) Field, L. M.; Lahti, P. M.; Palacio, F. *Chem. Commun.* **2002**, 636. (d) Field, L. M.; Lahti, P. M. *Inorg. Chem.* **2003**, *42*, 7447. (e) Luneau, D.; Romero, F. M.; Ziessel, R. *Inorg. Chem.* **1998**, *37*, 5078. (f) Fegy, K.; Lescop, C.; Luneau, D.; Rey, P. *Mol. Cryst. Liq. Cryst.* **1999**, *334*, 521.

Published on Web 08/14/2009

highly Lewis acidic $Mn(hfac)_2$ (hfac = 1,1,1,5,5,5-hexafluoroacetylacetonate) studied in the Gatteschi group.[4] Other neutral radical partners such as verdazyl were also examined, in some cases showing remarkably large couplings to metal centers,[5] but again mainly in isolated complexes or low dimensional arrays; Lemaire has recently published an excellent review of this area.[6] These early studies opened the door to the purposeful design of organic radicals as building blocks for self-assembled metal-organic magnetic materials.

To set up the cooperativity needed for spontaneous magnetization in a crystalline material, strong interspin couplings must be propagated through higher dimensionality (two- or three-dimensional, 2-D or 3-D) structurally defined networks.[1a] Thus, the ideal building block would be multitopic, able to bridge between tightly bound metal centers that, in turn, would contact multiple ligands. To avoid the insulating effects of diamagnetic anions or ligands (such as hfac) it would be anionic, providing intrinsic charge balance (and tighter binding) to the metal cation partners. And its geometrical relationship to the metal center would be firmly set via chelation.

Anionic radical building blocks built to this plan have recently yielded exciting results; benzimidazole substituted nitronyl nitroxide reacts with Mn(II) to form 2-D magnetic honeycombs with a T_c of 40 K.[7] Many other polynitrile anions and radical anions have been explored, especially tetracyanoquinodimethane (TCNQ) and tetracyanoethylene (TCNE).[8,9] Recently, Hicks[10] and Miller[11] have both reported compounds based on Ni(II) and either TCNQ or TCNE with above room-temperature magnetic ordering temperatures. Structural predictions remain difficult because of these components' weakly defined modes of coordination[12] with some notable exceptions.[13]

We have used the *o*-semiquinone radical anion as a model for the present work. Compounds such as 3,5-di-*tert*-butyl-*o*-semiquinone have chelating binding sites and bind readily to metals. The magnetic properties of these compounds have been studied extensively.[14] However, the simple semiquinone moiety lacks bridging abilities, so cannot propagate extended magnetic interactions. Covalent linking of semiquinone units with robust ferromagnetic couplers has been explored to overcome this shortcoming, but their organization into crystalline extended arrays remains elusive, presumably because of their stereochemical complexity.[15]

In our previous theoretical work,[16] mono- and dianions of tetrone **1** (Scheme 1, R = H) were proposed as new paramagnetic building blocks. The reasons for this choice are twofold: (a) Anions of **1** have a high probability of self-assembly into extended magnetic networks with well-defined cation-ligand geometric and magnetic interactions. Such motifs, which are formed by the isostructural diamagnetic dihydroxyquinone dianions, include molecular chains,[17] honeycomb sheets,[18] and even 3-D diamond-like networks.[19,20] In those self-assemblies, metal cations would be bridged and chelated by the anions of **1**. As with the closely related semiquinone complexes, coordination contacts can transfer strong magnetic couplings between the paramagnetic metal center and the ligands.[21] Radical anions of **1** may also be combined with

(4) (a) Caneschi, A.; Gatteschi, D.; Sessoli, R. *Inorg. Chem.* **1993**, *20*, 4612. (b) Caneschi, A.; Gatteschi, D.; Lelirzin, A. *J. Mater. Chem.* **1994**, *4*, 319. (c) Caneschi, A.; Gatteschi, D.; Sessoli, R. *Mol. Cryst. Liq. Cryst. Sci. Technol., Sect. A* **1996**, *278*, 177. (e) Caneschi, A.; Gatteschi, D.; Rey, P.; Sessoli, R. *Inorg. Chem.* **1991**, *30*, 3936.

(5) (a) Gilroy, J. B.; Koivisto, B. D.; McDonald, R.; Ferguson, M. J.; Hicks, R. G. *J. Mater. Chem.* **2006**, *16*, 2618. (b) Hicks, R. G.; Koivisto, B. D.; Lemaire, M. T. *Org. Lett.* **2004**, *6*, 1887. (c) Hicks, R. G. *Aust. J. Chem.* **2001**, *54*, 597. (d) Brook, D. J. R.; Lynch, V.; Conklin, B.; Fox, M. A. *J. Am. Chem. Soc.* **1997**, *119*, 5155. (e) Lemaire, M. T.; Barclay, T. M.; Thompson, L. K.; Hicks, R. G. *Inorg. Chim. Acta* **2006**, *359*, 2616.

(6) Lemaire, M. T. *Pure Appl. Chem.* **2004**, *76*, 277.

(7) Fegy, K.; Luneau, D.; Ohm, T.; Paulsen, C.; Rey, P. *Angew. Chem., Int. Ed.* **1998**, *37*, 1270.

(8) (a) Miller, J. S.; Epstein, A. J. *Chem. Commun.* **1998**, 1319. (b) Zhang, J.; Ensling, J.; Ksenofontov, V.; Gutlich, P.; Epstein, A. J.; Miller, J. S. *Angew. Chem., Int. Ed.* **1998**, *37*, 657. (c) Manriquez, J. M.; Yee, G. T.; McClean, R. S.; Epstein, A. J.; Miller, J. S. *Science* **1991**, *252*, 1415. (d) Jones, R. D.; Summerville, D. A.; Basolo, F. *J. Am. Chem. Soc.* **1978**, *100*, 4416. (e) Mikami, S.; Sugiura, K.; Maruta, T.; Maeda, Y.; Ohba, M.; Usuki, N.; Okawa, H.; Akutagawa, T.; Nisihara, S.; Nakamura, T.; Iwasaki, K.; Miyazaki, N.; Hino, S.; Asato, E.; Miller, J. S.; Sakata, Y. *J. Chem. Soc., Dalton Trans.* **2001**, 448.

(9) (a) Dunbar, K. R. *Angew. Chem.* **1996**, *35*, 1659. (b) Thompson, R. C.; Gujral, V. K.; Wagner, H. J.; Schwerdtfeger, C. F. *Phys. Status Solidi* **1979**, *53*, 181. (c) Clérac, R.; O'Kane, S.; Cowen, J.; Ouyang, X.; Heintz, R.; Zhao, H.; Bazile, M. J., Jr.; Dunbar, K. R. *Chem. Mater.* **2003**, *15*, 1840. (d) Bartley, S. L.; Bazile, M. J., Jr.; Clérac, R.; Zhao, H.; Ouyang, X.; Dunbar, K. R. *J. Chem. Soc., Dalton Trans.* **2003**, 2937.

(10) Jain, R.; Kabir, K.; Gilroy, J. B.; Mitchell, K. A. R.; Wong, K.; Hicks, R. G. *Nature* **2007**, *445*, 291.

(11) Miller, J. S.; Pokhodnya, K. I. *J. Mater. Chem.* **2007**, *17*, 3585.

(12) (a) Pokhodnya, K. I.; Petersen, N.; Miller, J. S. *Inorg. Chem.* **2002**, *41*, 1996. (b) Vickers, E. B.; Selby, T. D.; Thorum, M. S.; Taliaferro, M. L.; Miller, J. S. *Inorg. Chem.* **2004**, *43*, 6414. (c) Zhang, J.; Zhou, P.; Brinckerhoff, W. B.; Epstein, A. J.; Vazquez, C.; McLean, R. S.; Miller, J. S. *ACS Symp. Ser.* **1996**, *644*, 311.

(13) (a) Lopez, N.; Zhao, N.; Prosvirin, A. V.; Chouai, A.; Shatruk, M.; Dunbar, K. R. *Chem. Commun.* **2007**, 4611. (b) Miyasaka, H.; Izawa, T.; Takahashi, N.; Yamashita, M.; Dunbar, K. R. *J. Am. Chem. Soc.* **2006**, *128*, 11358. (c) Zhao, H.; Bacsa, J.; Prosvirin, A.; Lopez, N.; Dunbar, K. R. *Polyhedron* **2005**, *24*, 1907.

(14) (a) Buchanan, R. M.; Downs, H. H.; Shorthill, W. B.; Pierpont, C. G.; Kessel, S. L.; Hendrickson, D. N. *J. Am. Chem. Soc.* **1978**, *100*, 4318. (b) Buchanan, R. M.; Kessel, S. L.; Downs, H. H.; Pierpont, C. G.; Hendrickson, D. N. *J. Am. Chem. Soc.* **1978**, *100*, 7894. (c) Lynch, M. W.; Buchanan, R. M.; Pierpont, C. G.; Hendrickson, D. N. *Inorg. Chem.* **1981**, *20*, 1038. (d) Pierpont, C. G.; Attia, A. S. *Collect. Czech. Chem. Commun.* **2001**, *66*, 33. (e) Pierpont, C. G.; Buchanan, R. M. *Coord. Chem. Rev.* **1981**, *38*, 45. (f) Pierpont, C. G.; Lange, C. W. *Prog. Inorg. Chem.* **1993**, *41*, 381.

(15) (a) Shultz, D. A.; Boal, A. K.; Farmer, G. T. *J. Org. Chem.* **1998**, *63*, 9462. (b) Shultz, D. A.; Boal, A. K.; Driscoll, D. J.; Kitchin, J. R.; Tew, G. N. *J. Org. Chem.* **1995**, *60*, 3578. (c) Shultz, D. A.; Fico, R. M.; Lee, H.; Kampf, J. W.; Kirschbaum, K.; Pinkerton, A. A.; Boyle, P. D. *J. Am. Chem. Soc.* **2003**, 125 15426. (d) Shultz, D. A.; Fico, R. M.; Bodnar, S. H.; Kumar, R. K.; Vostrikova, K. E.; Kampf, J. W.; Boyle, P. D. *J. Am. Chem. Soc.* **2003**, *125*, 11761. (e) Caneschi, A.; Dei, A.; Mussari, C. P.; Shultz, D. A.; Sorace, L.; Vostrikova, K. E. *Inorg. Chem.* **2002**, *41*, 1086. (f) Shultz, D. A.; Kumar, R. K. *J. Am. Chem. Soc.* **2001**, *123*, 6431. (g) Shultz, D. A.; Bodnar, S. H.; Kumar, R. K.; Lee, H.; Kampf, J. W. *Inorg. Chem.* **2001**, *40*, 546. (h) Caneschi, A.; Dei, A.; Lee, H.; Shultz, D. A.; Sorace, L. *Inorg. Chem.* **2001**, *40*, 408.

(16) Misiolek, A. W.; Jackson, J. E. *J. Am. Chem. Soc.* **2001**, *123*, 4774.

(17) (a) Kawata, S.; Kitagawa, S.; Kumagai, H.; Kudo, C.; Kamesaki, H.; Ishiyama, T.; Suzuki, R.; Kondo, M.; Katada, M. *Inorg. Chem.* **1996**, *35*, 4449. (b) Decurtins, S.; Schmalle, H. W.; Zheng, L. M.; Ensling, J. *Inorg. Chim. Acta* **1996**, *244*, 165. (c) Kawata, S.; Kitagawa, S.; Kondo, M.; Katada, M. *Synth. Met.* **1995**, *71*, 1917. (d) Cueto, S.; Straumann, H. P.; Rys, P.; Petter, W.; Gramlich, V.; Rys, F. S. *Acta Crystallogr., Sect. C: Cryst. Struct. Commun.* **1992**, *48*, 458. (e) Robl, C.; Kuhs, W. F. *J. Solid State Chem.* **1989**, *79*, 46. (f) Robl, C. *Mater. Res. Bull.* **1987**, *22*, 1483. (g) Robl, C. *Z. Naturforsch., B* **1987**, *42*, 972. (h) Robl, C.; Weiss, A. *Mater. Res. Bull.* **1987**, *22*, 497. (i) Robl, C.; Weiss, A. *Z. Naturforsch., B* **1986**, *41*, 1337.

(18) Weiss, A.; Riegler, E.; Robl, C. *Z. Naturforsch., B* **1986**, *41*, 1501.

(19) Abrahams, B. F.; Coleiro, J.; Hoskins, B. F.; Robson, R. *Chem. Commun.* **1996**, 603.

(20) Ohrstrom, L.; Larsson, K. *Dalton Trans.* **2004**, 347–353.

(21) (a) Caneschi, A.; Dei, A.; Mussari, C. P.; Shultz, D. A.; Sorace, L.; Vostrikova, K. E. *Inorg. Chem.* **2002**, *41*, 1086. (b) Caneschi, A.; Dei, A.; Gatteschi, D.; Tangoulis, V. *Inorg. Chem.* **2002**, *41*, 3508. (c) Dei, A.; Gatteschi, D.; Sangregorio, C.; Sorace, L.; Vaz, M. G. F. *Inorg. Chem.* **2003**, *42*, 1701.

Scheme 1

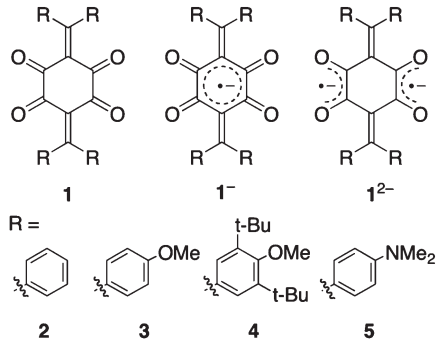

1 1^- 1^{2-} 2 3 4 5

diamagnetic cations. In this case, the high symmetry of the coordination spheres (e.g., 2-D honeycomb sheets[20]) should ensure high-spin coupling between neighboring ligands' unpaired electrons and thus favor ferromagnetic ordering in the solid.[22] (b) The highest occupied molecular orbital (HOMO)−lowest unoccupied molecular orbital (LUMO) gap of $\mathbf{1}^{2-}$ may be tuned by substitution on the methylene carbons and/or variation of the metal cation coordinated to the semidione sites. Our ab initio Multi Configuration Self Consistent Field (MCSCF) studies on derivatives of $\mathbf{1}^{2-}$ have found that electron-donating substituents R and coordination by highly charged metal cations can shrink the already small energy gap between these dianions' frontier orbitals, making them nearly degenerate. This degeneracy, coupled with the non-disjoint character of the frontier orbitals, leads to a calculated triplet preference of up to 4.5 kcal/mol for the coordinated dianion of **1**. This high-spin preference should make it possible to use the simple and more robust paramagnet $\mathbf{1}^-$ or the magnetically tunable $\mathbf{1}^{2-}$ depending on the preferred strategy.

This paper describes our efforts to experimentally test the predictions of our theoretical work via synthesis of substituted analogues of **1**, their structural characterization, and spectroscopic and electrochemical studies of their mono and dianions. It also offers preliminary insights into these building blocks' abilities to self-assemble into crystalline magnetically coupled radical-metal complex salts.

The parent tetrone framework **1** (R = H) is unlikely to survive even in neutral form, as it would be expected to polymerize readily. So the first experimental challenge was to synthesize derivatives of **1** with protecting groups that impart stability and a means of tuning the energy difference between the frontier molecular orbitals. The aryl-substituted tetrones **2**−**5** synthesized for this study (Scheme 1) meet these criteria. As with triarylmethyl radicals, the phenyl rings offer steric protection while substituents can be introduced to perturb the orbital energies. The radical anions and dianions of the parent and substituted tetrones in solution were prepared electrochemically and by alkali metal reduction and characterized by UV−vis−NIR absorption, electron paramagnetic resonance (EPR), and electron−nuclear double resonance (ENDOR) spectroscopies. Crystal structures of neutral tetrones **2** and **5** and the Na^+ and K^+ radical anion salts of **4** were obtained, and the salient features of their molecular structures will be described.

(22) (a) Pierpont, C. G.; Attia, A. S. *Collect. Czech. Chem. Commun.* **2001**, *66*, 33. (b) Pierpont, C. G.; Lange, C. W. *Prog. Inorg. Chem.* **1994**, *41*, 331. (c) Pierpont, C. G.; Buchanan, R. M. *Coord. Chem. Rev.* **1981**, *38*, 45.

Results and Discussion

Synthesis. Scheme 2 displays the general synthetic approach to **2**−**5**. A 2-fold electrophilic substitution of the diarylmethyl substituents onto the 2,5-dihydroxy-1, 4-benzoquinone core was achieved by sulfuric acid treatment of a mixture of the corresponding diarylmethanol and 2,5-dihydroxybenzoquinone in acetic acid. The resulting bis-diarylmethyl substituted dihydroxyquinones $\mathbf{2}H_4$−$\mathbf{5}H_4$ were then oxidized with the potent quinone oxidant dichlorodicyanoquinone (DDQ) in refluxing benzene or toluene to form the desired tetraaryl tetrones **2**−**5**, along with modest quantities of the half-oxidized product.

Scheme 2

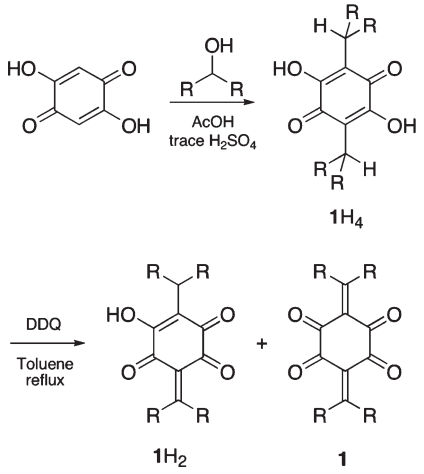

$\mathbf{1}H_4$ $\mathbf{1}H_2$ **1**

Electrochemistry. The redox behavior of **2** and its derivatives were investigated by means of cyclic voltammetry (CV). Figure 1 presents a voltammogram of **4** in tetrahydrofuran (THF) as a typical example. Two reversible reduction waves were observed, and the values of the measured reduction potentials for all tetrone derivatives

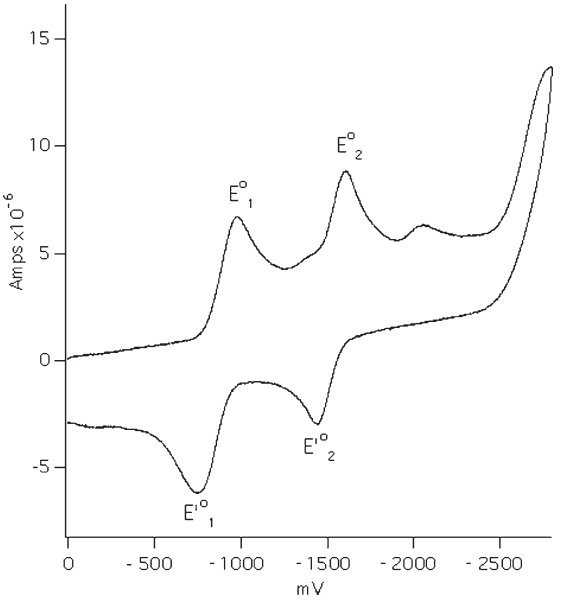

Figure 1. Cyclic voltammogram of **4** in THF (0.10 M $[(n\text{-Bu})_4N](PF_6)$) at room temperature and a scan rate of 0.1 V/sec.

Table 1. Reduction Potentials from Cyclic Voltammetry of 1 mM Solutions of Tetrones **2**−**5** with 0.1M of $(n\text{-Bu})_4N(PF_6)$ As Supporting Electrolyte

	$E_1°$	$E_2°$	$\Delta E_{1,2}°$
		THF	
2	−0.39	−1.10	0.71
4	−0.57	−1.22	0.65
		DMF	
2	−0.28	−0.91	0.63
3	−0.39	−0.96	0.57
5	−0.78	−1.27	0.49

(versus $E° = 0.46$ V for the ferrocene/ferrocinium couple) are collected in the Table 1.

The first wave corresponds to a one-electron reduction of the tetrone to its radical monoanion as confirmed by comparisons between spectroelectrochemical studies and UV−vis spectrophotometry (vide infra). These $E°$ values show the expected correlation with the electron-donating ability of the phenyl substituents: stronger donors shift the reduction potential of the tetrones to more negative values. The reduction potential $E_1°$ of **2** is less negative in DMF than in THF as expected; presumably the relative solvation of the anion versus neutral **2** is stronger in the more polar DMF. The oxidizing abilities of **2** and its derivatives are comparable to *p*- and *o*-benzoquinones measured under similar conditions (−0.43 V and −0.47 V for *p*-benzoquinone in DMF[24] and 3,5-di(*tert*-butyl)-*o*-quinone in THF[25] respectively).

The second wave $E_2°$ corresponds to the reduction of the monoanion to the dianion. Supporting this assignment, the values of the peak current, i_p, of $E_2°$ are close to those for $E_1°$. The separation between the first and the second reduction waves ranges from 0.49 to 0.63 V in DMF and points to the expected strong interactions between the two frontier orbitals in the dianion. The gap between the first two waves decreases with increasing electron-donating abilities of the phenyl ring substituents (0.63, 0.57, 0.49 V for **2**, **3**, **5** in DMF respectively). This observation correlates with ROHF triplet calculations on model compounds of $\mathbf{2}^{2-}$ that predict a decrease in the difference between the one-electron energies of the singly occupied frontier orbitals with increasing substituent donor abilities.[9] Hence, the electrochemistry is consistent with an open-shell biradical dianion as the product of the second reduction wave. There is a small irreversible wave present after the $E_2°$ peak that has been seen in electrochemical studies of similar quinone systems.[23] We attribute this peak to the reaction of $\mathbf{4}^{2-}$ with residual water present in the THF to form $\mathbf{4H}^-$, which can be further reduced.

The relative ease of reduction of uncoordinated **2** and $\mathbf{2}^-$ bodes well for preparation of complexes of mono and dianions by electron transfer from metallic centers to the neutral tetrone. It also ensures that, like semiquinone and catecholate anions in their numerous complexes, these systems will be compatible with a variety of transition metal cations.

(24) Almlof, J. E.; Feyereisen, M. W.; Jozefiak, T. H.; Miller, L. L. *J. Am. Chem. Soc.* **1990**, *112*, 1206.
(25) Bock, H.; Hierholzer, B.; Jaculi, D. *Z. Naturforsch., B* **1988**, *43*, 1247.
(23) Bauscher, M.; Mäntele, W. *J. Phys. Chem.* **1992**, *96*, 11101–11108.

Table 2. ENDOR-Determined Hyperfine Splitting Constants and Isotropic *g*-Values for Anions and Dianions of Tetrones **2**−**5** Prepared by Reduction in THF with Stoichiometric Quantities of Potassium and Cryptand[2.2.2]

radical anion	$a_1{}^a$(ortho)	$a_2{}^a$(meta)	$a_3{}^a$(para)	*g*-value
$\mathbf{2}^-$	±3.23	∓1.43	±3.23	2.0035
$\mathbf{3}^-$	±3.24	∓1.31	±0.36[b]	2.0032
$\mathbf{4}^-$	±3.39			2.0031
$\mathbf{5}^-$	±3.26	∓1.08		2.0030
$\mathbf{2}^{2-}$	±7.85	∓3.23	±7.85	2.0028
$\mathbf{4}^{2-}$	8.27			2.0028

[a] In MHz; 2.80 MHz = 1 Gauss. [b] *p*-methoxy protons.

EPR and ENDOR Studies of the Derivatives of $\mathbf{2}^-$ and $\mathbf{2}^{2-}$. Samples of radical anions and dianions for EPR and ENDOR spectroscopic studies were prepared by the reduction of tetrones, dissolved or suspended in THF, with alkali metal mirrors. To prepare "free anions", the macrobicyclic cryptand[2.2.2] (C222) was included in preparations involving potassium metal.[26] This powerful complexant forms a solution of potassium potasside ($K \cdot C222^+K^-$) and/or solvated electrons upon contact with a potassium mirror.[27] Either of these strong reducing agents may then reduce and dissolve substances that are themselves insoluble in THF (e.g., **3** and **5**). As expected, all monoanions were air sensitive. Under anaerobic conditions at room temperature, those with substituents in the *para* positions of the phenyl rings persisted without noticeable decomposition, but $\mathbf{2}^-$ decayed slowly ($t_{1/2} \sim$ 1 h) requiring temperatures below −20 °C to persist indefinitely. These results suggest that $\mathbf{2}^-$ tends to dimerize to form diamagnetic products, much like the closely related triarylmethyl radicals.[28]

All monoanions in solution showed X-band EPR signals with *g*-values characteristic for organic radicals (Table 2). The ^{1}H hyperfine splitting (hfs) constants a_n and their relative signs were determined by ENDOR and general triple ENDOR spectroscopies,[29] respectively, and are collected in Table 2. Figure 2 displays EPR and ENDOR spectra of $\mathbf{2}^-$ as a representative example. Experimental EPR spectra of the anion radicals were simulated by assigning values a_1 to the eight *ortho* (and for $\mathbf{2}^-$, the four *para*) protons and a_2 to the eight *meta* protons of the four phenyl groups. As expected for alternant hydrocarbons, a_1 and a_2 are opposite in sign. In general, simulations of high temperature ($T > 243$ K) solution EPR spectra based on ENDOR data show that the unpaired electron spin is delocalized over the entire molecule on the EPR time-scale. The hfs values are similar among derivatives of **2** showing that substituent effects do not affect the spin density significantly. In the absence of C222, hyperfine splitting to the alkali metal nucleus can be observed when **4** is reduced by Li (0.48 MHz) or Cs (0.5 MHz).

The dianion of **2** was prepared in several ways. The solution EPR spectrum shown in Figure 3 was obtained

(26) The IUPAC name for cryptand [2.2.2] is 4,13,16,21,24-hexaoxa-1,10-diazabicyclo-[8.8.8]hexacosane.
(27) Jedlinski, Z. *Acc. Chem. Res.* **1998**, *31*, 55.
(28) (a) McBride, J. M. *Tetrahedron* **1974**, *30*, 2009. (b) Jang, S.-H.; Gopalan, P.; Jackson, J. E.; Kahr, B. E. *Angew. Chem., Int. Ed. Engl.* **1994**, *33*, 775.
(29) Kurreck, H.; Kirste, B.; Lubitz, W. In *Electron Nuclear Double Resonance Spectroscopy of Radicals in Solution*; Marchand, A. P., Ed.; VCH: Weinheim, Germany, 1988.

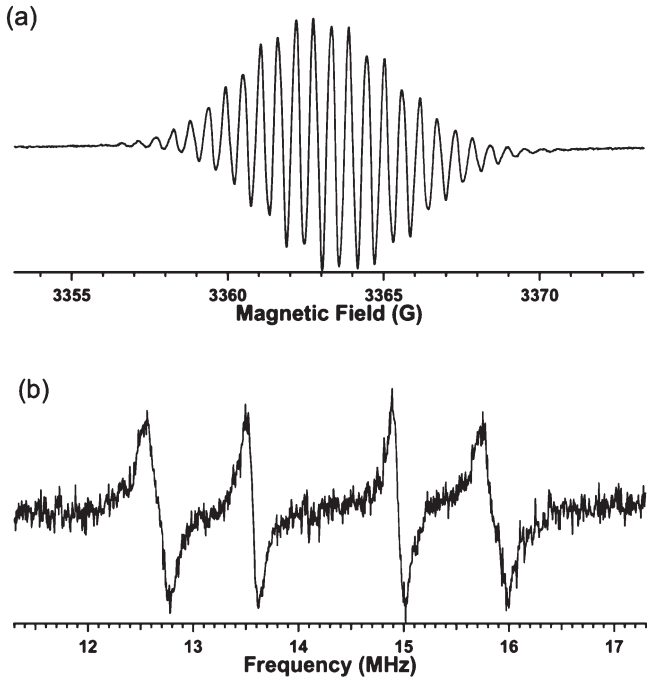

Figure 2. (a) EPR and (b) ENDOR spectra of **2** K·C222 in THF recorded at 246 K.

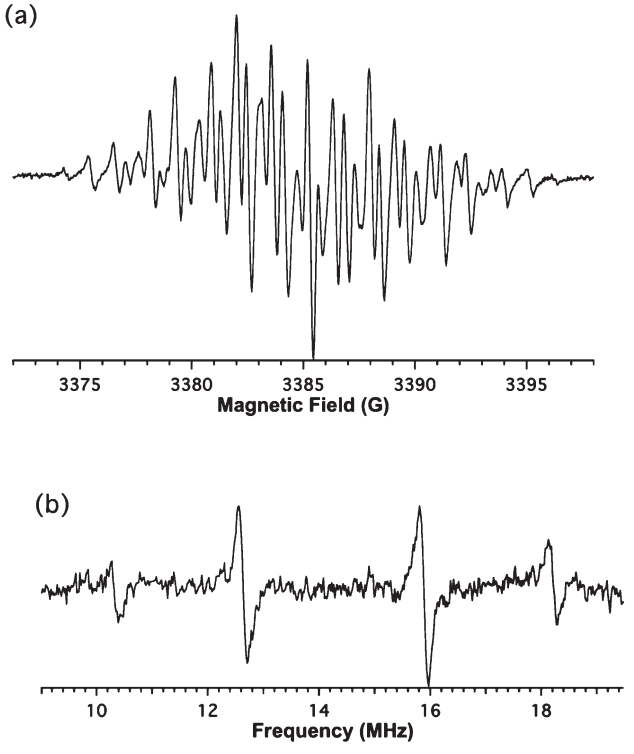

Figure 3. (a) EPR and (b) ENDOR spectra of **2**(K·[15-crown-5]$_2$)$_2$ in THF recorded at 223 K.

from the products of reaction of **2** with 2 equiv of potassium metal and 15-crown-5 in THF. On the basis of ENDOR measurements and simulation of the solution EPR spectra, the assignments of the hyperfine coupling constants are identical to those for the monoanion. However, the magnitude of the measured values is now twice that in the monoanion and corresponds to exactly

Scheme 3

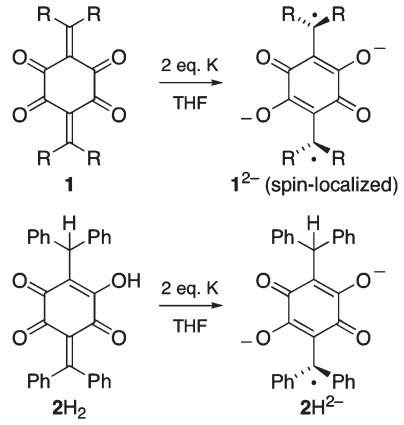

half the number of protons as verified by the spectral simulation. The dianion apparently behaves as a biradical in which each electron spin is localized to one of the diphenylmethyl termini.

To confirm that electron localization was a reasonable interpretation of the EPR spectrum, the monoradical dianion **2**H^{2-} was prepared from compound **2**H$_2$, an intermediate in the synthesis of tetrone **2**, using the same procedure as for the general preparation of diradical dianions **1**$^{2-}$ (see Scheme 3). This species exhibits a hfs pattern nearly identical to that seen for the dianion **2**$^{2-}$. Evidently, torsion about the C−C bonds connecting the two diarylmethyl subunits to the central $C_6O_4^{2-}$ ring effectively isolates the unpaired spins. The X-ray crystal structures of **2**, **5**, and two monoanion salts of **4** already show torsional angles of 30−40 degrees about these bonds (vide infra). While anions derived from hydrocarbons tend to have their charge and spin correlated, this connection breaks down when heteroatoms are involved.[30] The pinacol coupling[31] and the similarities in spin densities[32] between benzophenone ketyls $Ar_2CO^{-\bullet}$ and the corresponding triarylmethyl radicals $Ar_3C^{\bullet}$ are, in part, a consequence of this effect. Similarly, charge localization at oxygen sites in the dianions **1**$^{2-}$ because of strong association with the metal cations may displace spin density to the diarylmethylene subunits. With less delocalization than the monoanions, the dianions may be expected to have lower barriers to diarylmethyl twisting, consistent with the apparent electron localization seen here. This hypothesis is strengthened by the absence of hyperfine coupling to the metal cations Li^+ and Cs^+ in the solution EPR spectra of the dianions. The only evidence of minor contact density at Cs^+ is a broader line width relative to the **4**Li$_2$ adduct.

Frozen Solution Studies. A main goal of the EPR studies of the dianions was to determine their ground electronic states. The EPR spectra of frozen solutions of **4**Cs$_2$ and **4**Li$_2$ at 90 K are overlaid in Figure 4a. The lithium adduct exhibits what appears to be a triplet signal with very small zero field splitting (ZFS) accompanied by

(30) Fourré, I.; Silvi, B.; Chaquin, P.; Sevin, A. *J. Comput. Chem.* **1999**, *20*, 897.
(31) Smith, M. B.; March, J. *Advanced Organic Chemistry*; 5th ed.; Wiley: New York, 2001; pp 1559−1561.
(32) Jang, S.-H.; Mitchell, C.; Jackson, J. E.; Kahr, B. *Mol. Cryst. Liq. Cryst.* **1995**, *271*, A147.

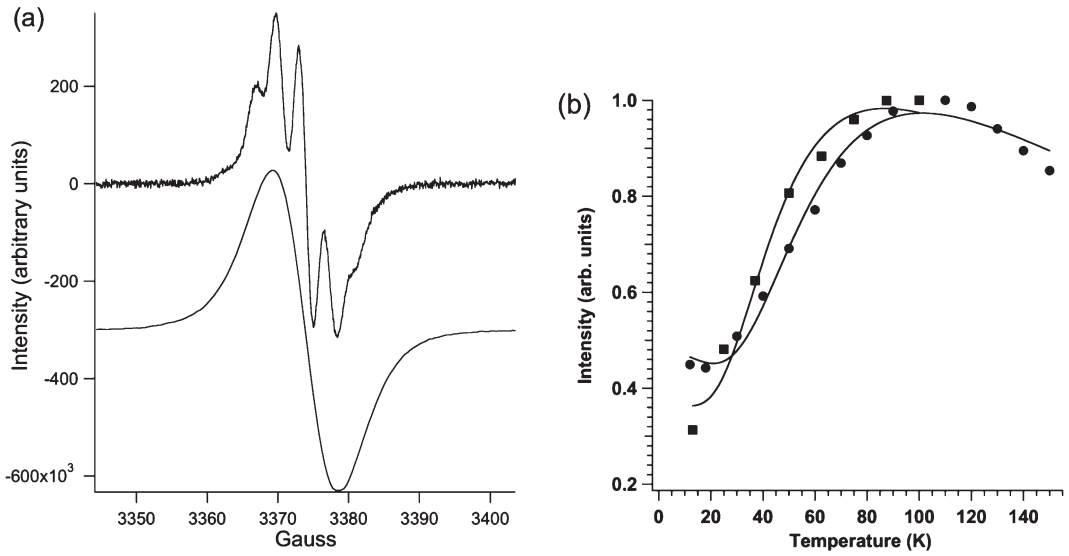

Figure 4. (a) EPR spectra of frozen solutions of $\mathbf{4}^{2-}$ obtained by reduction of **4** with 2 equiv of Li (top) and Cs (bottom) recorded at 90 and 75 K, respectively. (b) Temperature dependence of the EPR signal intensity of the thermally populated triplet states of $\mathbf{4}Li_2$ (circles) and $\mathbf{4}Cs_2$ (squares). The solid line correspond to fits to the Bleaney−Bowers expression. See text for further details.

a narrow monoradical signal. However, the intensity of *all* EPR signals increases as the temperature is raised and reaches a maximum at 110 K when Li^+ is the counterion. Since the apparent triplet and monoradical signals have the same temperature behavior, they must have a common origin. Hyperfine splitting to Li^+ is unlikely because the dianion solution spectrum shows negligible contact density at Li^+. Isotropic hyperfine coupling to four equivalent *ortho* hydrogens of the triarylmethyl fragments readily accounts for the line shape and temperature dependent behavior. The peak-to-peak distance is approximately 7.8 MHz, a value that is very close to what is observed in solution. It is noteworthy that the entire EPR spectrum of the lithium adduct fits within the envelope of the $\mathbf{4}Cs_2$ spectrum which is in agreement with the observation of broader linewidths in the $\mathbf{4}Cs_2$ solution spectrum.

The $\mathbf{4}Cs_2$ dianion has an intense central transition with a peak-to-peak line width of about 10 Gauss. The EPR intensity of the cesium adduct reaches a maximum at a slightly lower temperature, 85 K. Very weak sidebands with a separation of ~200 G can be observed with Cs^+ as the counterion, but these are likely due to intermolecular dimers formed through ion-pair association, as discussed below. A fit of the EPR intensity as a function of temperature between 4 and 150 K with a Bleaney−Bowers expression plus a Curie-law correction (Figure 4b) finds that the dianion diradicals have singlet ground electronic states with small exchange parameters of $2J = -97(14)$ and $-124(6)$ cm^{-1} for the cesium and lithium reduced tetrones, respectively.

The dianion prepared from the parent compound, $\mathbf{2}^{2-}$, yielded different powder pattern spectra depending on whether contact ion pairs were allowed to form in solution. A distinct triplet spectrum with $|D| = 0.0065$ cm^{-1} and a faint but characteristic half-field transition was observed when **2** was reduced with 2 equiv of potassium and 15-crown-5 in THF. Other metals and reducing agents yielded smaller $|D|$-values. However, when contact ion-pair formation was prevented by using potassium metal and C222 to prepare $\mathbf{2}^{2-}$, the EPR spectrum of the frozen solution consisted of a single line with $\Delta H_{pp} =$ 10 G. The temperature dependence of this signal indicated that $\mathbf{2}^{2-}$ has a singlet ground state. Unfortunately, the exchange parameter could not be reliably extracted from the data because of a monoradical signal with Curie-law behavior that offset the increase in the integrated intensities. Similar behavior was seen in the analysis of the frozen solution studies of $\mathbf{4}Li_2$. While it was not possible to simulate the spectrum shown in Figure 4a(top), an analysis of the line width places an upper limit on $|D|$ of 5×10^{-4} cm^{-1}. Nevertheless, it is clear that intermolecular dimers of $\mathbf{2}^{2-}$ are responsible for the triplet signals with modest ZFS and that these form readily with the parent compound and to a much lesser extent with the $\mathbf{4}Cs_2$ and $\mathbf{4}Li_2$ derivatives.

Electronic Spectroscopy. The tetrones and their anions were characterized by electronic spectroscopy. UV−vis (ultraviolet−visible) spectra in the range of 200−1000 nm were recorded for neutral tetrones in acetonitrile, while their reduction with *in situ* prepared K^+C222K^- in THF was monitored by vis−NIR (visible and near-infrared) spectroscopy in the 400−2000 nm range. These tetrones belong to an interesting group of molecules possessing conjugated electron-donor and electron acceptor moieties. Such systems are currently being investigated in the fields of nonlinear optics,[33] molecular electronics,[34] and artificial photosynthetic models.[35] The neutral tetrones show intense visible absorption bands (see Table 3) as well as the expected UV transitions. In the case of **2**, the two regions coalesce into a single band. The bathochromic shift in the visible absorption in the series **2**, **3**, and **5** reflects the increase in the electron-donating abilities of substituents in the order -H, -OMe, $-N(Me)_2$. Similar values can be seen in the case of p-substituted

(33) (a) Verbiest, T.; Houbrechts, S.; Kauranen, M.; Clays, K.; Persoons, A. *J. Mater. Chem.* **1997**, *7*, 2175. (b) Denning, R. G. *J. Mater. Chem.* **1995**, *5*, 365. (c) Nalwa, H. S. *Adv. Mater.* **1993**, *5*, 341.
(34) Metzger, R. M.; Panetta, C. A. *New J. Chem.* **1991**, *15*, 209.
(35) Kurreck, H.; Huber, M. *Angew. Chem., Int. Ed. Engl.* **1995**, *34*, 849.

Table 3. Electronic Absorption Maxima of Tetrones **2**−**5** and Their Mono- and Dianions

	λ_{max} (nm)		
tetrone	neutral (MeCN)	monoanion (THF)	dianion (THF)
2	354	430	485
		525	800
		1000	
3	498	530	745
	580 (shoulder)	600 (shoulder)	
		1100	
4	480	525	770
		610 (shoulder)	
		1150	
5	602	425	770
	674	635	
		1500	

diphenylmethyl carbocations (λ_{max} = 440 (-H), 507 (-MeO), 610 (-Me_2N) nm)).[36] The increase in donating ability not only changes the energy of the transition but also its intensity. The extinction coefficient of **5** is very high ($\sim 10^5$) making it an intense blue dye, while the absorptions of **3** and **2** (purple and red, respectively) are somewhat weaker. The charge-transfer band of **5** possesses two relatively close maxima at 602 and 674 nm. In **3**, this splitting is much less pronounced, and in addition to one maximum (498 nm) there is only a shoulder at 580 nm. Compound **2** has only one maximum (354 nm) but also a broad plateau which tails past 500 nm.

vis−NIR spectra of mono- and dianions of **2**−**5** prepared by reduction of tetrones with K^+C222K^- in THF show dramatic variations (see Table 3). To the eye, solutions of $\mathbf{2}^-$ are dark wine-red; $\mathbf{3}^-$ and $\mathbf{4}^-$ are purple (similar to aqueous solutions of permanganates), and $\mathbf{5}^-$ is green. In addition to the bands in the visible region, all monoanions possess a distinctive broad absorption band in the NIR region. Like the visible bands of the neutral tetrones, these transitions' energies decrease with increasing electron-donating power of the aryl substituents; peak maxima fall at 1000, 1100, 1150, and 1500 nm for $\mathbf{2}^-$, $\mathbf{3}^-$, $\mathbf{4}^-$, and $\mathbf{5}^-$, respectively. The correlation of the transition energy with the molecular structure suggests that the electron is excited from an orbital conjugated to the phenyl rings into another one that is relatively less affected by substitution. This assignment, supported by electrochemistry data (vide supra), validates the concept of frontier orbital gap tuning by substituent variation at the para sites on the phenyl rings.

The main absorptions in the vis−NIR spectra of the dianions are concentrated around 800 nm and are much less affected by the phenyl rings' substituents so the color of all dianion solutions is emerald-green. To confirm that the original tetrone framework was preserved through the two-electron reduction, a solution of dianion was prepared by reduction of **4** with 2 equiv of cesium metal in THF. Then, 2 days later, an additional equivalent of neutral **4** was added and the optical spectrum was recorded. Spectra identical to those of the directly prepared monoanion were observed, demonstrating the reversibility of electron addition and the robustness of the underlying structure.

(36) Deno, N. C.; Jaruzelski, J. J.; Schriesheim, A. *J. Am. Chem. Soc.* **1954**, *77*, 3044.

X-ray Diffraction Studies. Single crystals of neutral tetrones (**2** and **5**) and their monoanions (potassium and sodium salts of $\mathbf{4}^-$) were successfully grown and analyzed by X-ray diffraction. Key crystallographic data are summarized in Table 4. Selected bond lengths, OCCO core dihedrals, and propeller blade twist angles about the diarylmethylene carbons are presented in Tables 5−7, respectively.

Tetrone **2** crystallized from hot acetonitrile as dark red monoclinic needles in $P2_1/n$. The unique atoms of the unit cell comprise half of the tetrone molecule **2**, which contains an inversion center. Molecules of **2** are arranged in π stacks with an intermolecular separation equal to b (4.61 Å). Tetrone **5** crystallized from DMSO as dark blue blocks of $\mathbf{5}\cdot(DMSO)_3$. The unique atoms of the unit cell include one formula unit. Molecules of **5** are arranged into sheets with relatively short intermolecular contacts (O8−N37A 3.256 Å and O10−N27B 3.260 Å) between two of their carbonyl oxygens and nitrogen atoms of two neighboring tetrones. Additionally, two of its own nitrogen atoms (N37 and N27) interact in similar manner with carbonyl oxygens of another two neighbors. The difference between the packing modes of **2** versus **5** may be explained by the electrostatic polarization of the molecule because of transfer of charge between the electron-donating amine nitrogens and the electron-accepting carbonyl moieties. Intermolecular Coulombic interactions in the crystal of **5** also explain its relatively low solubility in nonpolar solvents. The geometries of single molecules of **2** and **5** are depicted in Figures 5 and 6. The central 3,6-dimethylene-1,2,4,5-tetraoxocyclohexane ring of **2** is puckered into a chairlike conformation, with the unique dicarbonyl dihedral OCCO angle being 26.9°. Similar deviations from planarity have been seen in [6]radialenes.[37] The tetrone ring of **5** is slightly different than that of **2**. Instead of adopting a pseudochair conformation, this molecule twists around the axis defined by the two methylene carbons. The values of the OCCO dicarbonyl dihedral angles (20.9° and 20.2°; see Table 6) are similar to those in **2**. Aryl and tetroxolane rings of **2** and **5** form a propeller-like arrangement. The steric and electronic differences between the phenyl rings and the tetrone core, which is formally doubly bonded to the methylene center, do not seem to greatly influence their respective out-of-plane twists. The twist angles defined by the mean planes of the four carbons of the "methylene centers" and the mean planes of the aryl and C_6O_4 rings are around 30°−40° (Table 7).

Slow diffusion of *n*-pentane into a THF solution of **4**K under oxygen-free conditions produced purple needle-like triclinic ($P\bar{1}$) crystals of $\mathbf{4}K\cdot(THF)_4$ with one molecule of the complex in the unit cell. A similar technique (using *n*-pentane/DME) produced crystals of $\mathbf{4}Na\cdot(DME)_4$ with the same color and symmetry but two unique molecules of **4** in the asymmetric unit. Figures 7 and 8 show the two structures, which both feature organic radical anions with planar central rings, in contrast to the puckered and twisted geometries seen in neutral compounds **2** and **5**. This result is sensible; population of a (previously empty) orbital with significant C−C π-bonding in the OCCO fragments should favor the planar geometry,

(37) Hopf, H.; Maas, G. *Angew. Chem., Int. Ed. Engl.* **1992**, *31*, 931.

Table 4. Selected Crystallographic Data for **2**, **5**·$(Me_2SO)_3$, **4**K·$(C_4H_8O)_4$, and **4**Na·$(C_6H_{10}O_2)_4$

	2	**5**·$(Me_2SO)_3$	**4**K·$(C_4H_8O)_4$	**4**Na·$(C_6H_{10}O_2)_4$
chem. formula	$C_{32}H_{20}O_4$	$C_{46}H_{58}N_4O_7S_3$	$C_{84}H_{124}O_{12}K$	$C_{168}H_{264}O_{32}Na_2$
fw	468.48	875.16	1364.99	2841.90
crystal system	monoclinic	monoclinic	triclinic	triclinic
space group	$P2_1/n$	$P2_1/n$	$P\bar{1}$	$P\bar{1}$
λ, Å (Mo Kα)	0.7107	0.7107	0.7107	0.7107
a, Å	13.8607(14)	21.092(4)	9.5055(2)	16.1411(4)
b, Å	4.6091(5)	8.0588(16)	13.0026(2)	16.3146(2)
c, Å	19.121(2)	26.781(5)	17.1668(2)	18.8482(4)
α, deg	90	90	77.2809(11)	64.4540(10)
β, deg	109.922(2)	101.31(3)	85.5001(12)	72.4140(10)
γ, deg	90	90	77.6417(10)	88.4470(10)
V, Å^3	1148.4(2)	4463.7(15)	2020.64(7)	4238.05(15)
Z	2	4	1	1
d_{calcd}, g cm^{-3}	1.355	1.302	1.384	1.114
μ, mm^{-1}	0.089	0.176	0.182	0.085
T, K	173(2)	293(2)	293(2)	293(2)
R	0.0493	0.0690	0.0844	0.0728
$R_{WF}2$	0.0952	0.1743	0.2430	0.2082
GOF	1.046	0.856	0.910	0.932

Table 5. Selected Bond Distances for Tetrones **2** and **5** and the Na^+ and K^+ Salts of the Monoanion of **4** (Bonds Labeled As Shown Below)

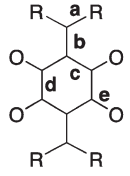

	2		**5**		**4Na**		**4K**	
a	C4−C5	1.480(3)	C11−C12	1.464(4)	C11−C12	1.481(9)	C7−C8	1.477(7)
	C4−C11	1.472(3)	C11−C21	1.453(4)	C11−C28	1.502(9)	C7−C28	1.465(8)
			C30−C31	1.458(4)	C44−C45	1.477(9)	C44−C45	1.482(7)
			C30−C40	1.475(4)	C44−C61	1.463(9)	C44−C61	1.457(8)
					C87−C88	1.490(9)		
					C87−C104	1.469(8)		
					C120−C121	1.482(8)		
					C120−C142	1.486(9)		
b	C3−C4	1.388(3)	C1−C11	1.440(4)	C2−C11	1.393(9)	C1−C44	1.440(8)
			C4−C30	1.429(4)	C5−C44	1.442(8)	C4−C7	1.398(8)
					C78−C87	1.442(8)		
					C81−C120	1.408(9)		
c	C1−C3A	1.471(3)	C1−C2	1.455(4)	C1−C2	1.478(8)	C1−C6	1.470(7)
	C2−C3	1.476(3)	C1−C6	1.459(4)	C2−C3	1.486(9)	C1−C2	1.434(8)
			C4−C3	1.464(4)	C4−C5	1.453(9)	C4−C5	1.464(9)
			C4−C5	1.477(4)	C5−C6	1.452(9)	C3−C4	1.449(7)
					C77−C78	1.457(8)		
					C78−C79	1.478(8)		
					C80−C81	1.479(9)		
					C81−C82	1.451(9)		
d	C1−C2	1.540(3)	C2−C3	1.559(4)	C1−C6	1.529(9)	C2−C3	1.547(8)
			C5−C6	1.545(5)	C3−C4	1.549(8)	C5−C6	1.492(8)
					C77−C82	1.512(9)		
					C79−C80	1.572(8)		
e	C1−O1	1.226(2)	C2−O7	1.240(4)	C1−O7	1.219(7)	C2−O25	1.236(7)
	C2−O2	1.212(2)	C3−O8	1.237(4)	C3−O10	1.207(7)	C3−O27	1.228(7)
			C5−O9	1.231(4)	C4−O9	1.258(7)	C5−O24	1.229(7)
			C6−O10	1.234(4)	C6−O8	1.263(8)	C6−O26	1.233(7)
					C77−O84	1.254(7)		
					C79−O85	1.228(7)		
					C80−O86	1.219(7)		
					C82−O83	1.245(8)		

as should the chelation of the alkali metal counterions by the carbonyl oxygens. Coordination of two anions about each cation leads to 1-D chains with the anions in the hoped-for chelating and bridging modes of coordination.

In **4**K each potassium cation in the chain forms a pseudo-cubic coordination sphere with four carbonyl oxygens from two tetrone molecules and four THF oxygens. The periodicity of the crystal implies that the central

Table 6. Selected Dihedrals for Tetrones **2** and **5** and the Na^+ and K^+ Salts of the Monoanion of **4** (Dihedral Angles Labeled As Shown Below)

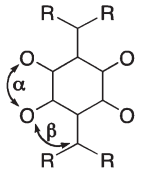

	2		**5**		**4K**		**4Na**	
α	O1−C1−C2−O2	26.9	O7−C2−C3−O8	−20.2	O24−C5−C6−O26	−1.7	O8−C6−C1−O7	8.2
			O9−C5−C6−O10	−20.9	O27−C3−C2−O25	3.6	O10−C3−C4−O9	−6.2
							O85−C79−C80−O86	7.8
							O83−C82−C77−O84	−6.8
β	O2−C2−C3−C4	−26.2	O10−C6−C1−C11	15.2	O24−C5−C4−C7	−0.8	O7−C1−C2−C11	−14.0
	O1A−C1A−C3−C4	37.6	C11−C1−C2−O7	10.4	C7−C4−C3−O27	−11.6	C11−C2−C3−O10	2.6
			O8−C3−C4−C30	8.4	O25−C2−C1−C44	2.1	O9−C4−C5−C44	14.4
			C30−C4−C5−O9	3.3	C44−C1−C6−O26	8.2	C44−C5−C6−O8	−5.3
							O86−C80−C81−C120	−3.5
							C120−C81−C82−O83	13.1
							O84−C77−C78−C87	6.5
							C87−C78−C79−O85	−16.9

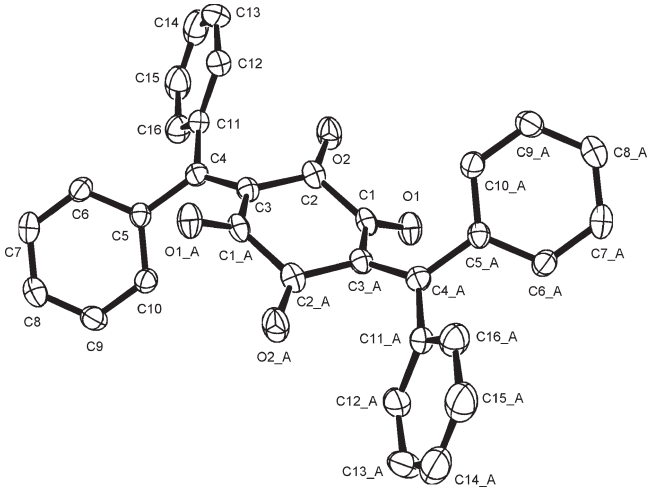

Figure 5. ORTEP drawing (50% probability) of **2**. Hydrogen atoms are omitted for clarity.

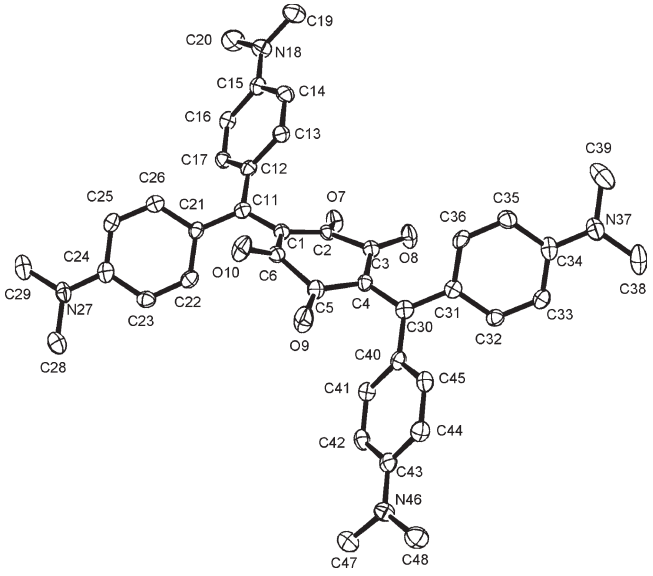

Figure 6. ORTEP drawing (50% probability) of **5**·$(Me_2SO)_3$. Hydrogen atoms and DMSO molecules are omitted for clarity.

Table 7. Angles of the Mean Ring Planes vs the Planes of the Diarylmethylene Centers in Tetrones **2** and **5** and the Na^+ and K^+ Salts of the Monoanion of **4**

2	C[3−5,11]	
C[5,10]	38.8	
C[11,16]	43.9	
C[1−3,1A−3A]	35.0	
5	C[4,30,31,40]	C[1,11,12,21]
C[40−45]	36.4	
C[31−36]	31.3	
C[1−6]	43.1	30.4
C[12−17]		34.0
C[21−26]		28.5
4K	C[4,18,28,7]	C[1,44,45,61]
C[8−13]	30.5	
C[28−30,35,38,43]	33.5	
C[1−6]	40.9	41.3
C[45−50]		34.6
C[61−6]		29.8
4Na (molecule 1)	C[2,11,28,12]	C[5,44,45,61]
C[12−17]	31.5	
C[28−33]	36.8	
C[1−6]	36.1	35.9
C[45−50]		38.6
C[61−6]		31.1
4Na (molecule 2)	C[78,87,88,104]	C[120,121,142,81]
C[88−93]	37.5	
C[104−109]	28.3	
C[77−82]	37.1	37.5
C[121−126]		28.2
C[137−142]		38.2

coordinating ring of all of the anions are parallel to each other. There is, however, a zigzag angle of 148.2° between the mean planes defined by the four oxygens of the tetrone rings and the four carbonyl oxygens coordinated to the potassium cation. The sodium salt's structure is qualitatively similar, but includes two independent alternating monoanions in the chain. The coordination sphere of the sodium cation (containing four tetrone oxygens and four oxygens of two chelated DME molecules) is also

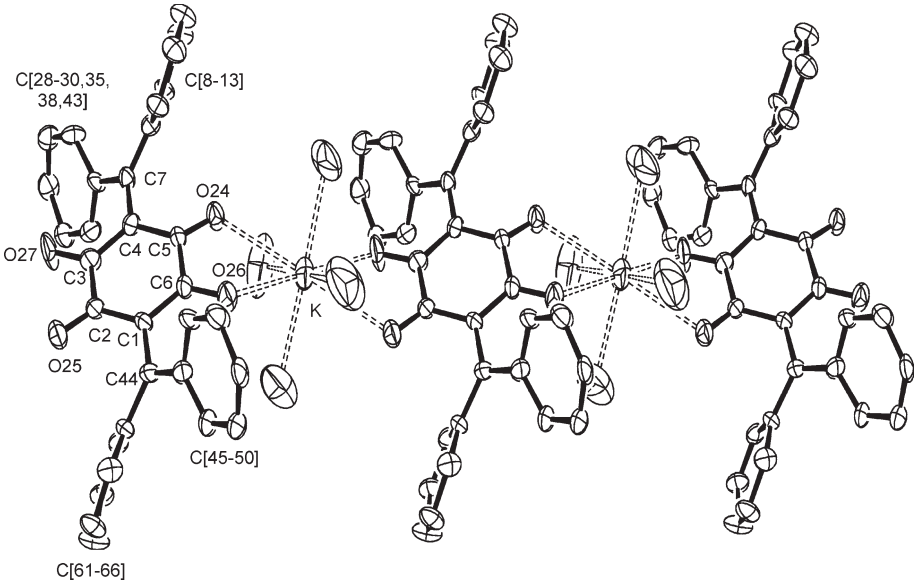

Figure 7. ORTEP drawing (50% probability) of chains formed in the solid state by radical anion salt $\mathbf{4}K\cdot(THF)_4$ with one unique molecule of complex. Hydrogen atoms, THF molecules (excluding coordinated oxygen atoms), and *t*-butyl and methoxy groups are omitted for clarity.

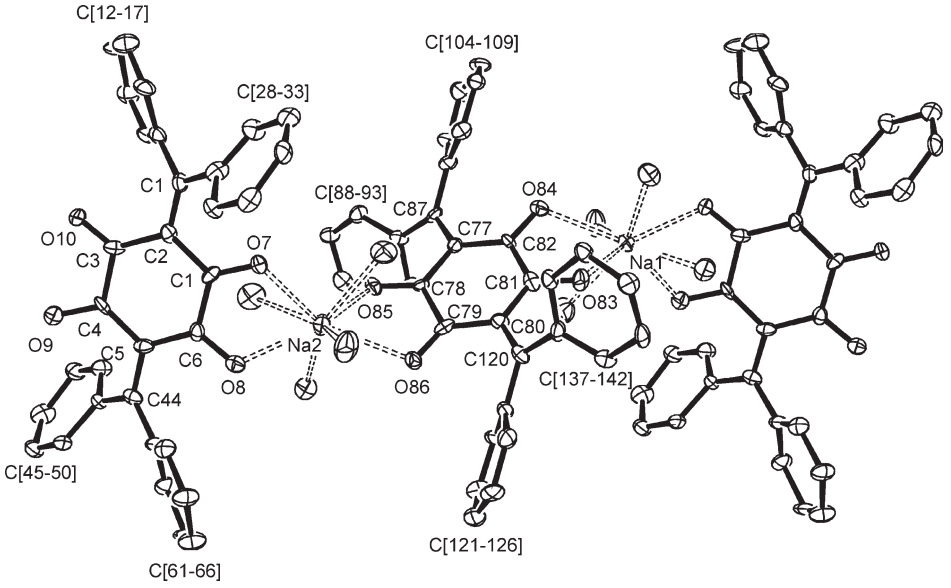

Figure 8. ORTEP drawing (50% probability) of chains formed in the solid state by radical anion salt $\mathbf{4}Na\cdot(DME)_4$ with two unique molecules of complex. Hydrogen atoms, DME molecules (excluding coordinated oxygen atoms), and *t*-butyl and methoxy groups are omitted for clarity.

distorted toward a square antiprism. This distortion rotates the planes of neighboring monoanions around the chain axis so that the angle between their central mean planes is 37.6°.

In addition to four unique coordinated molecules of DME there are also four non-coordinated ones located in the cavities between the chains. Some of them are quite disordered and not all of their hydrogens could be located. The similar modes of coordination found in both crystals confirm, as expected, that the negatively charged pocket formed by two oxygen atoms on one side of the anion is the preferred place for metal cation binding. That both potassium and sodium salts form 1-D chains may be attributed not only to the anions' design but also to the relatively low coordinating power of the solvents of crystallization. THF and DME are too weak as Lewis bases to compete with the chelating anions of **2**. A more polar or nucleophilic solvent might break the chains into separate ion aggregates. We have found such contrasting behaviors with the potassium radical anion salt of 2,3-bis(2-pyridyl)quinoxaline (dpq) which crystallized from THF as 1-D chains of $(dpq)K\cdot(THF)_2$ but from methylamine as discrete solvent separated ion-pair dimers of $(dpq)K\cdot(MeNH_2)_2$.[38] Despite repeated attempts, we have been unable to grow crystals of alkali metal salts of the dianions of **2** and its derivatives suitable for X-ray analysis. The metal-radical structures we have successfully crystallized to date are neutral without extra competing ions. Perhaps use of divalent alkaline earth or

(38) (a) Ichimura, A. S.; Szajek, L. P.; Xie, Q. S.; Huang, R. H.; Huang, S. Z.; Wagner, M. J.; Dye, J. L.; Jackson, J. E. *J. Phys. Chem. B* **1998**, *102*, 11029. (b) Ichimura, A. S.; Xie, Q.; Szajek, L. P.; Lema, J.; Burns, A.; Huang, R. H.; Jackson, J. E.; Dye, J. L. *J. Phys. Chem. A* **2000**, *104*, 3038.

transition metal cations will lead to the neutral chains of dianions. Alternatively, increasing the cation's charge might allow formation of 2-D networks based on chessboard or honeycomb motifs, without changing the internal neutralization.

Solid State Magnetic Studies. The magnetic susceptibility of crystalline $\mathbf{4}K\cdot(C_4H_8O)_4$ and $\mathbf{4}Na\cdot(C_4H_{10}O_2)_4$ were investigated with a SQUID magnetometer over the range 2−300K using a 1000 G field strength. Both solids are paramagnetic with weak spin−spin interactions. The best fits to the Curie−Weiss equation ($\chi = C/(T + \theta)$) yielded $\theta = -0.6$ K for sodium and $|\theta| < 0.1$ K for potassium salts. The obtained values of C were within experimental error equal to the theoretical ones. The strength of intermolecular spin coupling in $\mathbf{4}Na\cdot(C_4H_{10}O_2)_4$ was also assessed by fitting the magnetic data to Baker's model of the uniform chain interactions.[39] The fit yielded a coupling value of $2J/k = -0.2$ K. Although the couplings are very weak, they vary as expected based on cation size. In the sodium salt, where distances between metal separated carbonyl oxygens are in the range 4.02−4.52 Å, the magnetic coupling appears slightly stronger than in the potassium case (with analogous distances of 5.16−5.17 Å). Nevertheless for the purpose of assembly of molecule-based magnets these values are miniscule.

A recent combined polarized neutron diffraction and density functional study of a high-spin coupled Ti(IV) complex of Schiff-base diquinone radical ligands showed that moderate ferromagnetic coupling in this complex is mediated through spin delocalization over formally empty d orbitals of the cation rather than direct interaction of ligand-centered singly occupied molecular orbitals (SOMOs).[40] More electronically active diamagnetic cations should yield stronger couplings in our case as well. Another promising strategy is to assemble ferrimagnets by using paramagnetic cations to ensure direct contact between unpaired spins.

Conclusions and Outlook

On the basis of ab initio molecular orbital studies of diradical dianions with the 3,6-dimethylene-1,2,4,5-tetraoxocyclohexane skeleton, we have designed and synthesized compound **2** and three of its substituted derivatives. The structure, durability, and relative ease of handling of these organic molecules were confirmed. Structural studies have demonstrated a tendency toward assembly with metal cations into extended structures with bridging and chelating modes of coordination, the pivotal requirement for success of our long-range strategy. Spectroscopic and solution studies support the near degeneracy of the frontier orbitals as well as the tunability of their gap by methylene site substitution. Our calculations suggest that metal cation coordination analogous to that in the solid state chains of monoanions may tune the molecule to be a ground state triplet. Further work will explore main group and transition metal cations for this purpose. Although no evidence of strong electron coupling has appeared in the linear chain alkali metal salts of $\mathbf{4}^-$, we are confident that complexes of more highly charged diamagnetic and paramagnetic transition metal cations will display such behavior. In these cases interesting phenomena related to the ligand−metal electron transfer may be also anticipated.

Experimental Section

General Methods. Melting points were determined on a Thomas-Hoover apparatus and are uncorrected. ^{1}H and ^{13}C-{1H} spectra were obtained at 300 and 75.5 MHz, respectively on a Varian GEMINI 300 spectrometer. The ^{1}H and ^{13}C NMR shifts are referenced to residual ^{1}H and ^{13}C resonances of the deuterated solvents. 2,5-Dihydroxy-1,4-quinone, diphenylmethanol, bis(4-methoxyphenyl)methanol, bis(4-(dimethylamino)phenyl)methanol, and DDQ (2,3-dichloro-5,6-dicyano-1,4-benzoquinone) were purchased from Aldrich and used as received. C222 was vacuum sublimed and stored in a glovebox; $[(n\text{-}Bu)_4N](PF_6)$ was recrystallized three times from absolute ethanol and dried under vacuum. Bis(3,5-di-*tert*-butyl-4-methoxyphenyl)methanone was prepared according to literature methods.[41] Toluene and Et_2O were dried by refluxing over sodium/benzophenone under nitrogen; acetonitrile by refluxing over CaH_2 under nitrogen; all were freshly distilled before use. Other solvents were used as received. For the preparation, spectroscopic characterization, and crystal growth of anions, solvents were purified as follows. Anhydrous DME and THF were placed in a Schlenk bottle with a few drops of NaK alloy, degassed through a series of freeze−pump−thaw cycles, and left to sit until occasional shaking turned its color blue. The solvent was then freeze−pump−thawed until the vacuum over the frozen solid reached 10^{-5} torr. The solvent was then vacuum distilled to another Schlenk storage bottle. Just before the experiment, the required quantity of the solvent was distilled to a bottle containing a few drops of NaK, shaken until blue, and distilled into the K-Cell[42] apparatus where the experiments were conducted. Pentane was degassed and stored over NaK.

Cyclic Voltammetry. An amount the supporting electrolyte $[(n\text{-}Bu)_4N](PF_6)$ calculated to produce 0.1 M solution and a magnetic stirring bar was placed in a main chamber of an electrochemical cell equipped with a glassy carbon electrode, platinum wire counter-electrode, a freshly cleaned silver wire as a quasi-reference and a side arm. Before each experiment the carbon electrode was polished with an alumina paste, and sonicated. The required amount of tetrone was placed in the side arm of the cell to form about 1 mM solution. The cell was then evacuated on a high-vacuum line and about 2 mL of dry degassed THF was condensed into the main chamber. When anhydrous DMF was used as a solvent, it was transferred to the cell with a syringe inside a glovebag, and then degassed in the cell via several freeze−pump−thaw cycles. Cyclic voltammograms were recorded with EG&G Princeton applied research potentiostat/galvanostat and BAS CV-50W voltammetric analyzer. A sweep rate of 0.1 V/s was used in most cases and 100% IR compensation was achieved before each run. Before the tetrone was dissolved into the electrolyte solution, a few blank sweeps were done until no change in the background current could be seen. After the runs a small amount of ferrocene (Fc) was added to the solution in the glovebag to calibrate the potentials to the Fc/Fc^+ couple (0.46 V).

EPR, ENDOR and Electronic Spectroscopy. In a typical experiment, the tetrone (ca. 10 mg) and a small excess (ca. 1:2.2) of cryptand[2.2.2] were placed in one chamber of a K-cell with an EPR tube and a quartz optical cell attached. The cell was

(39) Baker, G. A.; Rushbrooke, G. S.; Gilbert, H. E. *Phys. Rev.* **1964**, *135A*, 1272.
(40) Pontillon, Y.; Bencini, A.; Caneschi, A.; Dei, A.; Gatteschi, D.; Gillon, B.; Sangregorio, C.; Stride, J.; Totti, F. *Angew. Chem., Int. Ed.* **2000**, *39*, 1786.
(41) Anderson, K. K.; Shultz, D. A.; Dougherty, D. A. *J. Org. Chem.* **1997**, *62*, 7575.
(42) Dye, J. L. *J. Phys. Chem.* **1984**, *88*, 3842.

evacuated on a high-vacuum line, and placed in a helium-filled glovebox. A small piece of potassium (ca. 5 mg) was placed in the rear chamber. The K-cell was then evacuated until the pressure was $< 10^{-5}$ torr. A potassium mirror was then prepared by heating the potassium with a small gas flame. The chamber containing the tetrone was immersed in liquid nitrogen, and THF (ca. 30 mL) was added. After dissolution of the tetrone, the K-cell was placed in an isopropanol/dry ice bath (−45 °C), and the solution was poured onto the metal mirror. The progress of reduction was monitored within the optical cell attached to the side arm with a Guided Wave Model 260 fiber-optic spectrophotometer. In some cases, dilution of the solution in the optical cell was necessary to keep the spectra on scale, so no extinction coefficients may be reported. A small amount of solution was transferred to the quartz EPR tube, the tube was sealed off, and the sample was held in liquid nitrogen until it could be analyzed by EPR and ENDOR. Spectra were recorded on a Bruker (9.5 GHz) ESP300E spectrometer equipped with a DICE ENDOR unit. Temperature was controlled with an Oxford Instruments 9000 liquid helium cryostat. The *g*-values were measured by determining the field and microwave frequency with a Bruker ERO35 M NMR gaussmeter and EIP model 25B frequency counter. Typical conditions for EPR were as follows: modulation frequency 100kHz, modulation amplitude 0.1 gauss, power 0.1mW, gain 10^5. Typical conditions for ENDOR were as follows: modulation frequency 12.5 kHz, microwave power 20−32 mW, radio frequency power 200−300 W, modulation depth 100 kHz, and gain 10^5. UV−vis spectra of the tetrones were recorded on a UNICAM UV2 in acetonitrile as the solvent.

Crystal Growth. Crystals of compound **2** were grown by slow cooling of an acetonitrile solution. Crystals of $\mathbf{5}\cdot((CH_3)_2SO)_3$ formed over time from a saturated DMSO solution of **5**. To produce crystals of $\mathbf{4}K\cdot(C_4H_8O)_4$, 50 mg of tetrone was dissolved in 30−50 mL of degassed THF and reacted with a potassium mirror following the procedure described for preparation of EPR samples. The solution of the potassium salt of this anion was then transferred to two 9 mm diameter Pyrex glass tubes attached to a K-cell. Pentane was condensed over the solution and allowed to diffuse for a couple of days in room temperature. Crystals of $4Na\cdot(C_4H_{10}O_2)_4$ were grown similarly but DME was used instead of THF.

SQUID Magnetometry. Approximately 5 mg samples of crystalline $\mathbf{4}K\cdot(C_4H_8O)_4$ and $\mathbf{4}Na\cdot(C_4H_{10}O_2)_4$ prepared as for X-ray studies were sealed into polyethylene bags in a Helium filled glovebox. The samples were promptly transferred into magnetometer (Quantum Design $MPMS_2$), and their magnetic susceptibility was investigated in the 2−300 K temperature range in a 1000 G magnetic field. The diamagnetic corrections were performed using the high temperature portion of the data.

Synthesis. Synthesis of **2** was accomplished in a two-step procedure (Scheme 2). Intermediate $\mathbf{2}H_4$ was prepared by refluxing an acetic acid solution of 2,5-dihydroxy-1,4-benzoquinone, diphenylmethanol, and a few drops of H_2SO_4. This reaction had a high yield (96%) of product that was convenient to isolate and purify. Of the many oxidizing agents that were tried in the next transformation, high-potential quinones (DDQ and *o*-chloranil) proved to be effective. Metal salts ($Pb(OAc)_4$, $K_3Fe(CN)_6$, $Ce(NH_4)_2(NO_3)_6$), and oxides (Ag_2O, activated MnO_2, PbO_2) did not react or formed insoluble and unreactive salts of $\mathbf{2}H_4$. Refluxing a solution of $\mathbf{2}H_4$ and DDQ in toluene led to a mixture of **2**, $\mathbf{2}H_2$, starting material, and other unidentified side products. Tetrone **2** was isolated from the reaction mixture by recrystallization, and its structure confirmed by X-ray crystallography. Intermediate $\mathbf{2}H_2$ was also isolated. Since ab initio calculations indicated that electron-donating substituents should stabilize the lowest triplet state of the diradical dianion relative to the lowest singlet, the electron donor-substituted derivatives of **2** displayed in Scheme 1 were also synthesized. Condensation of commercially available 4,4′-dimethoxybenzhydrol and 4,4′-bis(dimethylamino)benzhydrol with 2,5-dihydroxy-1,4-benzoquinone led to $\mathbf{3}H_4$ and $\mathbf{5}H_4$ under significantly milder conditions than required for $\mathbf{2}H_4$. Dehydrogenations were also much more facile for the substituted compounds. The shorter reaction times and the higher stability of the substituted tetrones minimized side reactions, thus increasing yields and simplifying workup procedures for **3** and **5**. The structure of the latter was also confirmed by X-ray crystallography. A new problem, however, arose with these substituted compounds. The presence of electron-donating substituents on the phenyl rings lowered the tetrones' solubility in organic solvents. To overcome this difficulty, an analogue of **3** with eight *t*-butyl groups attached to the phenyl rings in the meta positions (**4**) was prepared in a similar fashion.

$\mathbf{2}H_4$. A 2 g portion of 2,5-dihydroxy-1,4-benzoquinone (14.3 mmol), 5.5 g of diphenylmethanol (29.9 mmol), and 0.5 mL of conc. H_2SO_4 were refluxed for 1 h in 20 mL of acetic acid and then left at room temperature to cool. The crystalline mass obtained was crushed with a spatula and vacuum-filtered through a glass frit. The collected yellow crystals were washed with a small amount of acetic acid and then thoroughly washed with water. Crystals were dried overnight at about 90 °C in air giving 6.5 g (96.5%) of orange powder. The purity of the resulting $\mathbf{2}H_4$ proved to be sufficient for the next step. It could, however, be recrystallized from 20 mL of acetic acid giving 6 g (89% yield) of the product: mp 190−192 °C, ^{1}H NMR ($CDCl_3$, 300 MHz): $\delta = 5.69$ (s; 1 H), 7.2−7.3 (m; 10 H), 7.95 (s; 1 H), ^{13}C NMR ($CDCl_3$, 75 MHz): $\delta = 45.6$, 117.3, 126.75, 128.4, 129.0, 140.6 (broadening caused by rapid proton shifts makes it difficult to detect signals of the quaternary C=O and C−OH carbons).

$\mathbf{2}H_2$. $\mathbf{2}H_4$ (6 g, 12.7 mmol), DDQ (1 g, 4.4 mmol), and benzene (30 mL) were gently refluxed with magnetic stirring for 18 h under a nitrogen atmosphere. The benzene was evaporated, 75 mL of $CHCl_3$ were added to the flask, and after a few minutes of stirring at room temperature, the solution was suction filtered. The separated solid of 2,3-dichloro-5,6-dicyano-1,4-hydroquinone was washed with more $CHCl_3$, and the combined chloroform solutions were evaporated to dryness. After the addition of 25 mL of acetic acid to the flask, the solution was refluxed until the entire solid was dissolved. It was then left to cool. The precipitated $\mathbf{2}H_4$ (which can be reused) was filtered off and washed with more acetic acid. The combined acetic acid solutions were concentrated under vacuum to a dark red oil, cold water was added, and the mixture stirred until the oil solidified. The resulting orange-brown solid of crude $\mathbf{2}H_2$ was filtered off, washed with water, and dried. The dry solid was then crushed, refluxed with 800 mL of cylohexane for about 25 min, and the solution was cooled, filtered, and concentrated to about 80 mL of volume. The precipitated orange crystals of $\mathbf{2}H_2$ (1.2 g, 58%yield based on DDQ) were filtered off, dried, and once again recrystallized from cyclohexane; mp 115−116 °C (dec.), ^{1}H NMR ($CDCl_3$, 300 MHz): 5.93 (s; 1 H), 7.1−7.6 (m; 20 H), 8.0−8.2 (broad; 1H), ^{13}C NMR ($CDCl_3$, 75.5 MHz): 46.3, 126.8, 128.0, 128.4, 129.1, 131.4, 132.1, 132.6, 140.3, 140.9, 157.4, 177.2, 179.4, 180.3.

2. A 10 g portion of $\mathbf{2}H_4$ (21.2 mmol), 10 g of DDQ (44.1 mmol), and 70 mL of dry benzene were gently refluxed with stirring for 24 h under a nitrogen atmosphere, the solvent was evaporated, and the solid washed with about 200 mL of Et_2O and air-dried. The resulting red powder was dissolved in 200 mL of $CHCl_3$ and filtered. The separated solid $DDQH_2$ was washed with more $CHCl_3$ and combined chloroform solutions were concentrated to about 25 mL. When 300 mL of Et_2O was poured into the concentrate, after a while red crystals of crude **2** separated. The product was purified by recrystallization from hot acetonitrile (yield 2−10%); mp 288−290 °C (dec.), ^{1}H NMR ($CDCl_3$, 300 MHz): 7.2−7.6 (m; 20 H), ^{13}C NMR ($CDCl_3$, 75.5

MHz): 128.1, 132.0, 132.5, 140.0, 180.1, 186.6. Analysis: calcd C 82.0%, H 4.3%, exp. C 81.04%, H 4.55%.

3H$_4$. To the well-stirred refluxing solution of 2 g of 2,5-dihydroxy-1,4-benzoquinone (14.3 mmol) in 100 mL of acetic acid containing a few drops of conc. H_2SO_4 was added 7.0 g (28.7 mmol) of bis(4-methoxyphenyl)methanol. The solution first became red and after a while a yellow product precipitated. The suspension obtained was refluxed for about 15 min more, cooled to room temperature and filtered. The collected powder was washed first with acetic acid, then water, and dried giving 8 g (13.5 mmol 94.4%) of crude product which was recrystallized from dioxane; mp = 263−4 °C, ^{1}H NMR (DMSO-d$_6$, 300 MHz): δ = 3.71 (s; 6 H), 5.46 (s; 1 H), 6.82 (d; J = 8.7 Hz, 4 H), 7.07 (d; J = 8.7 Hz, 4 H), 11 (broad; 2 H), ^{13}C NMR (DMSO-d$_6$, 75.5 MHz): δ = 43.4, 55.0, 113.5, 118.0, 129.6, 133.9, 157.5.

3. A 1.3 g portion of **3**H$_4$ (2.2 mmol) and 1 g of DDQ (4.4 mmol) were refluxed in 50 mL of toluene for 3 h. The solvent was evaporated, and the solid extracted in a Soxhlet extractor with 100 mL of CH_2Cl_2. The resulting dark purple solution of tetrone was diluted with 100 mL of Et_2O, left aside for about 1 h and filtered giving 0.9 g (70%) of product: mp > 300; ^{1}H NMR ($CDCl_3$, 300 MHz): δ = 3.87 (s; 3 H), 6.88 (d; J = 10 Hz, 2 H), 7.28 (d; J = 10 Hz, 2 H), Analysis: calcd C73.5%, H 4.8%, found C 72.52%, H 5.06%.

5H$_4$. A 2 g portion of 2,5-dihydroxy-1,4-benzoquinone (14.3 mmol) and 7.8 g (28.9 mmol) of 4,4′-bis(dimethylamino)-benzhydrol was refluxed with stirring in 100 mL of absolute EtOH for 15 min, the solution was cooled, and the purple product of spectroscopic purity (8.7 g, 13.5 mmol, 94.3%) filtered off, washed with ethanol, and dried: mp = 169−170 °C (dec.), ^{1}H NMR ($CDCl_3$, 300 MHz): δ = 2.90 (s; 12 H), 4−4.5 (broad; 1 H), 5.49 (s; 1 H), 6.64 (d; J = 9 Hz, 4 H), 7.10 (d; J = 9 Hz, 4 H), ^{13}C NMR ($CDCl_3$, 75.5 MHz): δ = 40.7, 43.8, 112.5, 117.7, 129.6, 129.75, 148.9, 168.4.

5. To a well-stirred solution of 1 g (1.55 mmol) of **5**H$_4$ dissolved in 100 mL of CH_2Cl_2 was added slowly 0.7 g (3.1 mmol) of DDQ dissolved in 100 mL of $CHCl_3$. During addition the solution turned dark blue. It was left stirring for about 20 min more, and the solvent was removed by evaporation. Separation of the product from $DDQH_2$ was achieved on a glass frit by slow dissolution of the protonated product with conc. HCl until the acid was no longer yellow. The resulting acidic solution was neutralized first with NaOH and then with sodium bicarbonate until the solution reached pH 7−8. The precipitated blue suspension of product was suction filtered, washed with water, dried, and recrystallized from hot DMSO giving 0.9 g (67%) of **5**·$((CH_3)_2SO)_3$: mp > 300 (dec.), ^{1}H NMR (DMSO-d$_6$, 300 MHz): δ = 3.13 (s; 12 H), 6.76 (d; J = 9 Hz, 4 H), 7.20 (d; J = 9 Hz, 4 H). Analysis: calcd C 63.1%, H 6.7%, N 6.4%; found C 62.43%, H 6.94%, N 6.61%.

Bis(3,5-di-*tert*-butyl-4-methoxyphenyl)methanol. To a well-stirred suspension of 30 g (71.7 mmol) of bis(3,5-di-*tert*-butyl-4-methoxyphenyl)methanone in 250 mL of methanol, was slowly added 7 g of $NaBH_4$. During the process the mixture warmed up, became homogeneous, and started to froth. When the reaction slowed down it was refluxed for about 30 min more. After cooling, 250 mL of water was added, and the milky solution was extracted with three 100 mL portions of CH_2Cl_2. The combined extracts were dried over Na_2SO_4 and evaporated to dryness. The waxy residue was recrystallized from a small volume of hexanes giving 26 g of the product: mp = 115−116.5, ^{1}H NMR ($CDCl_3$, 300 MHz): δ = 1.38 (s; 36 H), 2.2 (s broad; 1 H), 3.66 (s; 6 H), 5.72 (s; 1 H), 7.22 (s; 4 H), ^{13}C NMR ($CDCl_3$, 75.5 MHz): δ = 32.0, 35.8, 64.2, 76.7, 125.1, 137.6, 143.4, 158.8.

4H$_4$. To a well-stirred refluxing suspension of 1.4 g of 2,5-dihydroxy-1,4-benzoquinone (10 mmol) in 100 mL of acetic acid containing a few drops of conc. H_2SO_4 was added 10.0 g (21.3 mmol) of bis(3,5-di-*tert*-butyl-4-methoxyphenyl)methanol. The solution was refluxed for about 15 min, 40 mL of water was added, and the mixture was cooled to room temperature and filtered. The collected yellow crystals were washed first with water, then methanol, and dried giving 10 g (9.7 mmol, 97%) of crude product which was recrystallized from acetic acid: mp = 232−3 °C, ^{1}H NMR ($CDCl_3$, 300 MHz): δ = 1.36 (s; 72 H), 3.68 (s; 12 H), 5.51 (s; 2 H), 7.11 (s; 8 H), 8 (s broad; 2 H), ^{13}C NMR ($CDCl_3$, 75 MHz): δ = 32.1, 35.7, 45.2, 64.1, 117.9, 127.2, 134. 8, 142.9, 157.9.

4. A 4.6 g portion of **4**H$_4$ (4.425 mmol), 2 g of DDQ (8.8 mmol), and 50 mL of dry toluene were gently refluxed with stirring for 5 h. The hot solution was filtered, and the filtrate evaporated to dryness. The resulting dark red solid was triturated with two 50 mL portions of hexane giving the crude product which was recrystallized from toluene/hexane giving 2.6 g (56%) of tetrone: mp > 300 (dec.), ^{1}H NMR ($CDCl_3$, 300 MHz): δ = 1.35 (s; 36 H), 3.71 (s; 6 H), 7.15 (s; 4 H), ^{13}C NMR ($CDCl_3$, 75 MHz): δ = 31.9, 35.8, 64.6, 129.8, 133.3, 134.5, 143.1, 165.0, 178.4, 184.2. Analysis: calcd C 78.7%, H 8.9%; found C 77.77%, H 9.58%.

Acknowledgment. The authors gratefully acknowledge partial support for AWM and VPM via grants DMR-9610335 and DMR-9988881 to J.E.J. and Professor James L. Dye. Thanks are also due to Dr. Dimitris Papoutsakis for initial crystallographic instruction and data analyses and to Professor David A. Shultz of North Carolina State University for insightful discussions.

Supporting Information Available: UV/vis, EPR, and ENDOR spectra; crystallographic tables for each structure, including (a) crystal data; (b) atomic coordinates; (c) bond lengths and angles; (d) anisotropic displacement parameters; and (e) hydrogen coordinates. In addition, the .cif data files are available. This material is available free of charge via the Internet at http://pubs.acs.org.